Fingerprinting Brownian Motions of Polymers under Flow

Zhiqiang Shen, Jan-Michael Y. Carrillo, Bobby G. Sumpter, and Yangyang Wang*
Center for Nanophase Materials Sciences, Oak Ridge National Laboratory, Oak Ridge, Tennessee 37831, USA

(Received 7 March 2022; accepted 8 July 2022; published 28 July 2022)

We present a quantitative approach to the self-dynamics of polymers under steady flow by employing a set of complementary reference frames and extending the spherical harmonic expansion technique to dynamic density correlations. Application of this method to nonequilibrium molecular dynamics simulations of polymer melts reveals a number of universal features. For both unentangled and entangled melts, the center-of-mass motions in the flow frame are described by superdiffusive, anisotropic Gaussian distributions, whereas the isotropic component of monomer self-dynamics in the center-of-mass frame is strongly suppressed. Spatial correlation analysis shows that the heterogeneity of monomer self-dynamics increases significantly under flow.

DOI: 10.1103/PhysRevLett.129.057801

Polymeric liquids exhibit complex and fascinating flow behavior [1]. Despite the remarkable theoretical progress brought about by the tube model [2–4], understanding the molecular dynamics of long-chain molecules under flow still faces formidable challenges. In particular, little is known about how the tube diameter and number of entanglements—key theoretical constructs in models of entangled polymers—change under flow [5–11]. Moreover, characterizations of these quantities in computer simulations often rely on *ad hoc* algorithms [12–20], whose validity cannot be unequivocally demonstrated in the *deformed state*. Any direct attack on this problem must confront the microscopic nature of polymer entanglements, which is yet to be firmly established in the equilibrium state, let alone the nonequilibrium state.

To circumvent this theoretical difficulty and provide a solid phenomenological basis for understanding the nonequilibrium dynamics of polymers under flow, we turn our attention to density self-correlation functions, which are fundamental and well-defined quantities for describing liquid dynamics [21]. Despite numerous attempts in the past to characterize the self-motions of complex fluids under flow [22–32], an effective and systematic approach has not emerged. Here, we outline a quantitative method for analyzing the density self-correlation of polymers under steady flow by extending the spherical harmonic expansion technique [33–37] to dynamic density correlation functions. A key idea is to examine the polymer self-dynamics in two complementary coordinates: the center-of-mass (c.m.) motions in the *flow frame* and the segmental motions in the *c.m. frame*. Application of this approach to nonequilibrium molecular dynamics (NEMD) simulations permits a direct, quantitative analysis of anisotropic self-correlations, unveiling a number of universal features. First, the c.m. displacements of polymer melts in the flow frame follow a superdiffusive anisotropic Gaussian distribution with the mean-squared displacement (MSD) $\tilde{g}_{\rm cm} \sim t^{\gamma}$ $(1 < \gamma < 2)$, as a result of the interchain interactions in response to the imposed deformation. Second, the isotropic component of monomer self-dynamics in the c.m. frame is strongly suppressed under flow. Lastly, flow significantly increases the dynamical heterogeneity of monomer self-dynamics, as manifested by enhanced long tails of the self-correlation function. These observations hold true for both unentangled and entangled polymers, over a broad range of strain rates, correlation times, and length scales.

Our technical approach comprises three essential ingredients. First, we note that a direct analysis of the self-intermediate scattering function or self-correlation function under flow in the *laboratory frame* is difficult, due to the position-dependent convection effect [23,24,38,39]. Additionally, simple convection correction protocols based on a single reference frame [23,25,27,29] (e.g., the "SLLOD frame" of c.m.) are inadequate for fully addressing the nonequilibrium dynamics of polymers. To properly decompose the polymer self-dynamics under flow, we introduce two complementary coordinate systems (Fig. 1) as a generalization of the single reference frame idea. One is the *flow frame*, where the c.m. position $\tilde{\mathbf{R}}^{\alpha}_{\rm cm}(t)$ of a polymer chain α relative to the flow field (frame) after an elapsed time t is described by $\tilde{\mathbf{R}}^{\alpha}_{\rm cm}(t) \equiv \mathbf{R}^{\alpha}_{\rm cm}(t) - \int_0^t \nabla\mathbf{v}\cdot\mathbf{R}^{\alpha}_{\rm cm}(t')\mathrm{d}t'$, with $R^{\alpha}_{\rm cm}(t)$ being the c.m. position in the laboratory frame and $\nabla\mathbf{v}$ being the average velocity gradient tensor. The other is the *polymer c.m. frame*, in which the position $\hat{\mathbf{R}}^{\alpha}_{j}(t)$ of segment j of chain α relative to the c.m. is $\hat{\mathbf{R}}^{\alpha}_{j}(t) \equiv \mathbf{R}^{\alpha}_{j}(t) - \mathbf{R}^{\alpha}_{\rm cm}(t)$. The self-intermediate scattering functions of c.m. motions in the flow frame $\tilde{F}_{\rm cm}(\mathbf{Q},t)$ and monomer motions in the polymer c.m. frame $\hat{F}_{\rm mon}(\mathbf{Q},t)$ are therefore respectively defined as follows:

$$\tilde{F}_{\rm cm}(\mathbf{Q},t) = \frac{1}{M}\sum_{\alpha=1}^{M}\langle \exp\{-i\mathbf{Q}\cdot[\tilde{\mathbf{R}}^{\alpha}_{\rm cm}(t) - \tilde{\mathbf{R}}^{\alpha}_{\rm cm}(0)]\}\rangle, \quad (1)$$

$$\hat{F}_{\mathrm{mon}}(\mathbf{Q},t)=\frac{1}{MN}\sum_{\alpha=1}^{M}\sum_{j=1}^{N}\langle\exp\{-i\mathbf{Q}\cdot[\hat{\mathbf{R}}_j^{\alpha}(t)-\hat{\mathbf{R}}_j^{\alpha}(0)]\}\rangle, \tag{2}$$

where M is the number of polymer chains and N the chain length. For a homogeneous flow $\nabla\mathbf{v}$, $\tilde{F}_{\mathrm{cm}}(\mathbf{Q},t)$, and $\hat{F}_{\mathrm{mon}}(\mathbf{Q},t)$ provide a complete description of polymer self-dynamics in the nonequilibrium state. In the real space, two complementary self-correlation functions $\tilde{G}_{\mathrm{cm}}(\mathbf{r},t)$ and $\hat{G}_{\mathrm{mon}}(\mathbf{r},t)$ can be defined as $\tilde{G}_{\mathrm{cm}}(\mathbf{r},t)\equiv(2\pi)^{-3}\times\int\tilde{F}_{\mathrm{cm}}(\mathbf{Q},t)e^{i\mathbf{Q}\cdot\mathbf{r}}\mathrm{d}\mathbf{Q}$ and $\hat{G}_{\mathrm{mon}}(\mathbf{r},t)\equiv(2\pi)^{-3}\int\hat{F}_{\mathrm{mon}}(\mathbf{Q},t)\times e^{i\mathbf{Q}\cdot\mathbf{r}}\mathrm{d}\mathbf{Q}$, in the flow and c.m. frames, respectively. It should be emphasized that this work focuses on the self-dynamics under steady flow (i.e., $t=0$ starts from the steady state), as opposed to transient space-time correlations.

The second major technical ingredient concerns the quantification of anisotropic self-intermediate scattering functions $\tilde{F}_{\mathrm{cm}}(\mathbf{Q},t)$ and $\hat{F}_{\mathrm{mon}}(\mathbf{Q},t)$. To bypass the difficulty of directly analyzing these quantities in a high-dimensional space, we employ the spherical harmonic expansion technique [33–37], which has so far only been applied to anisotropic static structural correlations, to decompose the self-intermediate scattering function $F_{\mathrm{s}}(\mathbf{Q},t)$:

$$F_{\mathrm{s}}(\mathbf{Q},t)=\sum_{l,m}F_{l,m}(Q,t)Y_{l,m}(\theta,\phi), \tag{3}$$

where $Y_{l,m}(\theta,\phi)$ is the spherical harmonic function of degree l and order m, and $F_{l,m}(Q,t)$ is the corresponding expansion coefficient. $F_{l,m}(Q,t)$ condenses the information of anisotropic space-time correlations and is more amenable to analysis. Similarly, the self-correlation functions $\tilde{G}_{\mathrm{cm}}(\mathbf{r},t)$ and $\hat{G}_{\mathrm{mon}}(\mathbf{r},t)$ can also be expanded by spherical harmonics, and the corresponding coefficients $G_{l,m}(r,t)$ can be computed either directly or from the reciprocal space coefficients using spherical Bessel transform [40].

Lastly, we extend the notion of spatial correlation analysis of intermediate scattering functions in the equilibrium state [41] to the nonequilibrium state. Specifically, the spatial dependence of expansion coefficients $F_{l,m}(Q,t)$ and $G_{l,m}(r,t)$ are explored at fixed correlation times. This is generally a more fruitful way of analyzing dynamic correlation functions than the traditional method of examining time correlations at constant wave numbers [41].

We apply the aforementioned approach to study the self-dynamics of polymer melts under steady extensional flow using NEMD simulations of a coarse-grained bead-spring model [42,43]. All the beads interact with a purely repulsive Lennard-Jones potential, and the bonded interactions between neighboring beads along the polymer chain are described by the FENE potential, $U_{\mathrm{FENE}}=-\frac{1}{2}kR_0^2\ln[1-(r/R_0)^2]$, with $R_0=1.5$ and $k=30$. The chain stiffness is controlled by a bond bending potential $U_{\mathrm{bend}}(\alpha)=k_\alpha(1+\cos\alpha)$, where α is the angle between two subsequent bonds and $k_\alpha=1.5$. We consider polymer melts of four different chain lengths $N=20$, 40, 300, and 500 at density $\rho=0.85$ and temperature $T=1$. The equilibrium entanglement length of the model under such conditions is $N_{\mathrm{e}}\approx 28$ [43]. Homogeneous uniaxial extensional flow is imposed by integrating the SLLOD equations [44] with the generalized Kraynik-Reinelt boundary conditions [45,46]. The flow rate can be measured by the dimensionless Rouse-Weissenberg number $\mathrm{Wi}_{\mathrm{R}}=\dot{\varepsilon}\tau_{\mathrm{R}}$, with the Rouse relaxation time $\tau_{\mathrm{R}}=\tau_0N^2$ [47]. The self-dynamics of each system in steady state are examined after Hencky strain $\varepsilon=5$. All the simulations were performed with the GPU-accelerated LAMMPS package [49–51], and additional details can be found in the Supplemental Material [52].

To illustrate the basic idea of our technical approach, a representative result for the $N=300$ melt is given in Fig. 1. The leading spherical harmonic expansion coefficients of the self-intermediate scattering functions defined in the flow and c.m. frames [Eqs. (1) and (2)] are computed and presented as 2D color maps. It is worth noting that for the uniaxial extension symmetry, only the even-degree and

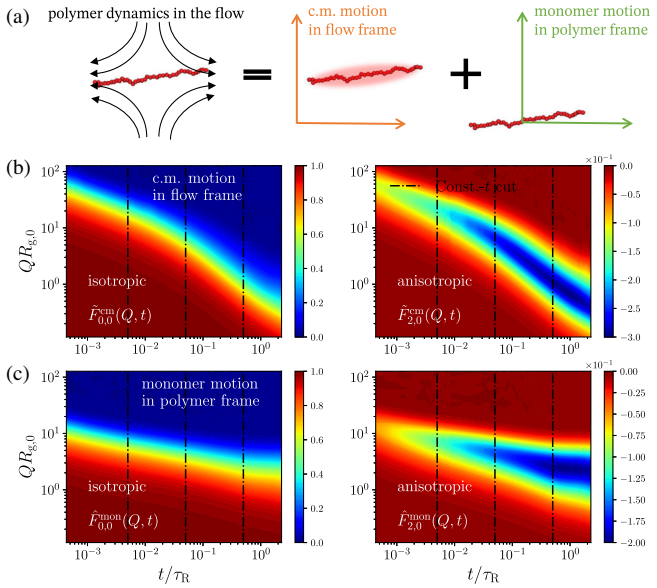

FIG. 1. (a) Illustration of the two reference frames for decomposing polymer self-dynamics under flow. (b) Two-dimensional color maps of the spherical harmonic expansion coefficients $\tilde{F}^{\mathrm{cm}}_{0,0}(Q,t)$ and $\tilde{F}^{\mathrm{cm}}_{2,0}(Q,t)$ of the c.m. self-intermediate scattering function $\tilde{F}_{\mathrm{cm}}(\mathbf{Q},t)$ in the flow frame. The wave number Q is scaled by the radius of gyration $R_{\mathrm{g},0}$ in the equilibrium state. (c) Coefficients $\hat{F}^{\mathrm{mon}}_{0,0}(Q,t)$ and $\hat{F}^{\mathrm{mon}}_{2,0}(Q,t)$ of the monomer self-intermediate scattering function $\hat{F}_{\mathrm{mon}}(\mathbf{Q},t)$ in the c.m. frame. The dashed lines indicate cuts of the 2D maps at fixed correlation times. The results given here are based on NEMD simulations of the $N=300$ system under steady extensional flow of $\mathrm{Wi}_{\mathrm{R}}=\dot{\varepsilon}\tau_{\mathrm{R}}=3$, with τ_{R} being the Rouse time.

zero-order terms appear in the spherical harmonic expansion [36]. To further characterize these expansion coefficients, we perform spatial correlation analysis by focusing on the Q dependence of $F_{l,0}(Q,t)$ at constant correlation times t.

The results for the c.m. self-dynamics in the flow frame are shown in Fig. 2. Before analyzing the behavior of $\tilde{F}_{\rm cm}(\mathbf{Q},t)$, we first examine the c.m. MSD $\tilde{g}_{\rm cm}$ in the flow frame, which is the second moment of $\tilde{G}_{\rm cm}(\mathbf{r},t)$, or equivalently $-\nabla_{\mathbf{Q}}^2\tilde{F}_{\rm cm}(\mathbf{Q},t)$ at $Q=0$ [23]:

$$\tilde{g}_{\rm cm}=\frac{1}{M}\sum_{\alpha=1}^{M}\langle[\mathbf{R}_{\rm cm}^{\alpha}(t)-\mathbf{R}_{\rm cm}^{\alpha}(0)-\int_0^t\nabla\mathbf{v}\cdot\mathbf{R}_{\rm cm}^{\alpha}(t')\mathrm{d}t']^2\rangle. \tag{4}$$

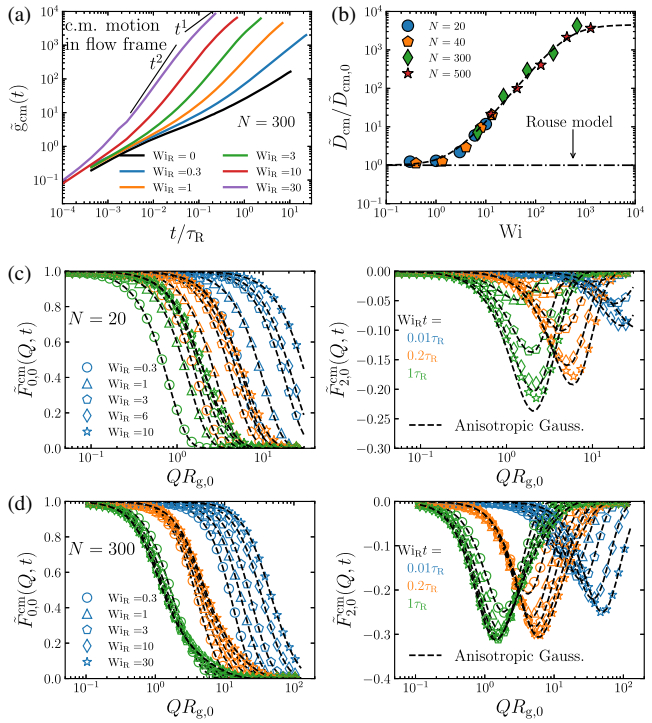

FIG. 2. Center-of-mass motions of the $N=20$ and $N=300$ melts in the flow frame. (a) c.m. mean-squared displacements $\tilde{g}_{\rm cm}(t)$ relative to the flow field. (b) Relative change of diffusivity $\tilde{D}_{\rm cm}/\tilde{D}_{\rm cm,0}$ with the Weissenberg number Wi. $\tilde{D}_{\rm cm,0}$ is the diffusivity without flow. $\mathrm{Wi}\equiv\dot{\epsilon}\tau_{\rm chain}$, with $\tau_{\rm chain}$ being the chain relaxation time. The dashed line is a guide for the eye. The dash-dotted line indicates the prediction of the Rouse model. (c) Spherical harmonic expansion coefficients $\tilde{F}^{\rm cm}_{0,0}(Q,t)$ and $\tilde{F}^{\rm cm}_{2,0}(Q,t)$ of the c.m. self-intermediate scattering function $\tilde{F}_{\rm cm}(\mathbf{Q},t)$ of the $N=20$ system at different correlation times t and Rouse-Weissenberg numbers $\mathrm{Wi_R}$. The results of the same $\mathrm{Wi_R}$ are represented by the same symbol. Furthermore, the data of the same normalized correlation time $\mathrm{Wi_R}t$ are shown in the same color. The dashed lines show anisotropic Gaussian fits of the expansion coefficients according to Eq. (5) with no adjustable parameters. (d) Results for the $N=300$ melts.

Due to the symmetry of uniaxial extensional flow, $\tilde{g}_{\rm cm}=\sum_\beta\tilde{g}^{\beta}_{\rm cm}$, where $\beta=x,\ y,\ z$, and $\tilde{g}^{\beta}_{\rm cm}$ is the MSD in the direction β. In the long-time limit, $\tilde{g}_{\rm cm}$ exhibits normal diffusive behavior, $\tilde{g}_{\rm cm}\sim\tilde{D}_{\rm cm}t$, where the apparent c.m. diffusivity $\tilde{D}_{\rm cm}$ increases with increasing extension rate. The relative change of c.m. diffusivity $\tilde{D}_{\rm cm}/\tilde{D}_{\rm cm,0}$ is found to be controlled by the Weissenberg number Wi, and the data from different chain lengths can be collapsed onto a master curve [Fig. 2(b)]. While the Rouse model (with the prediction of $\tilde{D}_{\rm cm}\sim\mathrm{Wi}^0$) undoubtedly fails to describe the behavior of the unentangled chains, it is unclear at this point whether any models for entangled polymers envision the master curve in Fig. 2(b). On the other hand, superdiffusive behavior is observed on intermediate timescales: $\tilde{g}_{\rm cm}\sim t^{\gamma}$ $(1<\gamma<2)$. Most interestingly, the spherical expansion technique allows a detailed examination of the functional form of $\tilde{F}_{\rm cm}(\mathbf{Q},t)$. We find that the c.m. self-intermediate scattering function in the flow frame can be described by an anisotropic Gaussian function:

$$\tilde{F}_{\rm cm}(\mathbf{Q},t)=\exp\left(-\frac{1}{2}\sum_{\beta}\tilde{g}^{\beta}_{\rm cm}Q_{\beta}^2\right). \tag{5}$$

Equation (5) can be verified by examining the spherical harmonic expansion coefficients of $\tilde{F}_{\rm cm}(\mathbf{Q},t)$. Figures 2(c) and 2(d), and additional results in the SM [52] confirm that Eq. (5) is valid for both unentangled and entangled melts, over a wide range of extension rates, wave numbers, and correlation times.

These findings point to a critical role of interchain interactions in polymer melt dynamics—effects that have not been adequately addressed in current theoretical models. To qualitatively understand our results, let us consider a Langevin equation for the c.m. motion of chain α: $\zeta(\dot{\mathbf{R}}_{\rm cm}^{\alpha}-\nabla\mathbf{v}\cdot\mathbf{R}_{\rm cm}^{\alpha})=\mathbf{f}^{\alpha}+\mathbf{f}_{\rm B}^{\alpha}$, where ζ is the friction coefficient, $\mathbf{f}^{\alpha}$ is the conservative force exerted on chain α by other chains, and $\mathbf{f}_{\rm B}^{\alpha}$ is the stochastic Brownian force. It is easy to see that in the absence of $\mathbf{f}^{\alpha}$ (e.g., the Rouse model), the self-correlation $\tilde{G}_{\rm cm}(\mathbf{r},t)$ of c.m. motions in the flow frame follows an isotropic, diffusive Gaussian function. Furthermore, we note that the simple convection-diffusion equation for a single particle under flow yields superdiffusive, anisotropic Gaussian self-dynamics in the laboratory frame [22,23,52,63,64], as a result of the coupling between normal diffusion and convection. Analyzing the c.m. self-motions in the flow frame removes the convection contribution $\nabla\mathbf{v}\cdot\mathbf{R}_{\rm cm}^{\alpha}$. However, an analogous coupling between the displacement due to interchain forces $\mathbf{f}^{\alpha}$ and diffusion should be responsible for the superdiffusive, anisotropic Gaussian dynamics in the flow frame. Such a conclusion is further supported by the force analysis and colloidal simulations presented in the Supplemental Material [52]. For equilibrium dynamics, the lack of a

proper treatment of intermolecular forces, particularly the effective interactions between centers of mass, in the classical mean-field theories of polymer dynamics [3] has long been recognized [65,66]. The current observations speak to the necessity of considering this issue for nonequilibrium dynamics. Conversely, our technical approach provides a direct and quantitative way of examining the effect of interchain forces on the c.m. dynamics in steady flow.

Having analyzed the c.m. motions in the flow frame, we now turn our attention to the monomer self-dynamics in the c.m. frame. Our analysis focuses on the isotropic components $\hat{F}^{\rm mon}_{0,0}(Q,t)$ and $\hat{G}^{\rm mon}_{0,0}(r,t)$ of the self-correlations. Figure 3(a) displays representative 2D color maps of $\hat{F}^{\rm mon}_{0,0}(Q,t)$ of the $N=300$ melt. With increasing extension rate, the contour lines of $\hat{F}^{\rm mon}_{0,0}(Q,t)$ systematically shift towards higher Q, implying a *suppression* of isotropic monomer self-dynamics by the flow. To better portray this trend, the contour lines of $\hat{F}^{\rm mon}_{0,0}(Q^*,t)=e^{-1}$ are shown in Fig. 3(b) for the $N=20$ and $N=300$ melts at various extension rates. Q^* defines a characteristic length scale $\xi(t)\equiv 1/Q^*$ for the segmental fluctuations within the c.m. frame at a given correlation time, which is approximately $R_{g,0}/\sqrt{3}$ for $t\to\infty$ in the quiescent state [3]. It is evident from Fig. 3(b) that the monomer self-dynamics of both

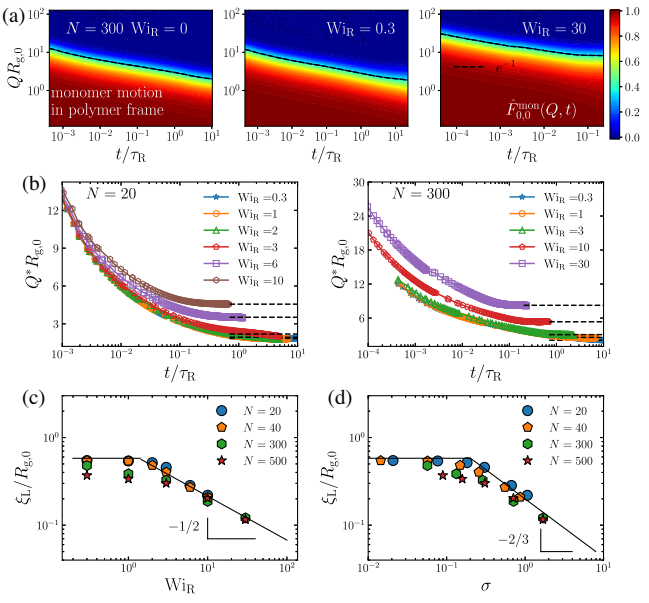

FIG. 3. Monomer motions in the c.m. frame. (a) Two-dimensional color maps of the isotropic expansion coefficient $\hat{F}^{\rm mon}_{0,0}(Q,t)$ of the self-intermediate scattering function $\hat{F}_{\rm mon}(\mathbf{Q},t)$ at equilibrium, $\mathrm{Wi_R}=0.3$, and $\mathrm{Wi_R}=30$. The dashed lines are contour lines of $\hat{F}^{\rm mon}_{0,0}(Q^*,t)=e^{-1}$. (b) Characteristic wave number $Q^*R_{g,0}$ at various Rouse-Weissenberg numbers for the $N=20$ and $N=300$ melts. (c) Rate dependence of the characteristic length scale in the long-time limit ξ_L. (d) Dependence of ξ_L on the steady-state tensile stress σ.

unentangled and entangled melts are suppressed by flow over a wide range of correlation times. To further quantify this effect, we present the limiting characteristic length scale at long time, $\xi_L\equiv\lim_{t\to\infty}\xi(t)$, as a function of the Rouse-Weissenberg number $\mathrm{Wi_R}$ and the steady-state tensile stress $\sigma\equiv\sigma_{zz}-(\sigma_{xx}+\sigma_{yy})/2$ in Figs. 3(c) and 3(d), respectively. ξ_L decreases monotonically with increasing $\mathrm{Wi_R}$, and σ and exhibits the asymptotic behavior of $\xi_L\sim\mathrm{Wi_R}^{-1/2}$ and $\xi_L\sim\sigma^{-2/3}$ at high strain rates.

It is interesting to ask whether changes of polymer entanglements under flow can be inferred from the monomer self-dynamics in the c.m. frame. The observed suppression of isotropic segmental fluctuations (Fig. 3) is consistent with the general theoretical expectation of the reduction of tube diameter under deformation [5,9,10]. Incidentally, the scaling relation $\xi_L\sim\sigma^{-2/3}$ coincides with the dependence of tube diameter on tension force predicted in Ref. [9]. However, the suppression effect revealed by our analysis is present in both unentangled and entangled melts, and it involves a broad range of timescales. In other words, the underlying physics here appears to be more generic. To understand the origin of the suppressed fluctuations, we performed Brownian dynamics simulations of both free and constrained Rouse chains [52]. Our calculations show that chain orientation and stretching is not the direct cause for the fluctuation suppression, suggesting that the driving force behind this phenomenon is also intermolecular in nature. Similar to the c.m. self-dynamics discussed previously, addressing the observed suppressed monomer self-dynamics under flow requires a proper treatment of the collective dynamics of polymers.

Lastly, our approach permits a quantitative analysis of the heterogeneity of polymer self-dynamics, which in the equilibrium state manifests as a long tail in the self-correlation function [67]. Figure 4 compares the isotropic component $\hat{G}^{\rm mon}_{0,0}(r,t)$ of the c.m. frame self-correlation function $\hat{G}_{\rm mon}(\mathbf{r},t)$ of the $N=300$ melt at equilibrium and $\mathrm{Wi_R}=10$. In both cases, the tail of the spatial correlation deviates from the Gaussian distribution and displays an exponential-like long tail at large r: $\hat{G}^{\rm mon}_{0,0}(r,t)\sim\exp[-r/\lambda(t)]$. The presence of flow significantly prolongs the tail of the distribution, leading to enhanced dynamical heterogeneity. The changes of $\lambda(t)$ of the $N=20$ and $N=300$ melts under flow are shown in Figs. 4(c) and 4(d) (additional results for $N=40$ and $N=500$ can be found in the Supplemental Material [52]). While the flow increases the heterogeneity of self-dynamics in both cases, the effect is much more pronounced for the entangled system ($N=300$). At this point, we are unaware of any theoretical models that qualitatively capture the behavior depicted in Figs. 4(c) and 4(d). Nevertheless, the physical origin of the observed heterogeneity enhancement can be intuitively appreciated: for entangled polymers $\lambda(t)$ can be interpreted as a characteristic *dynamic* length scale associated with the

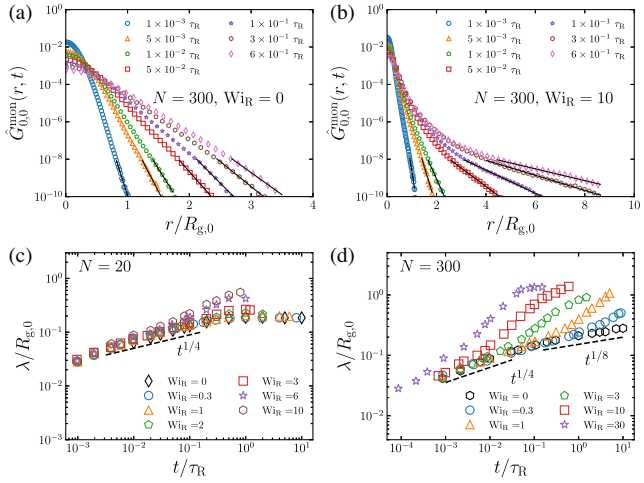

FIG. 4. (a) Isotropic component $\hat{G}^{\mathrm{mon}}_{0,0}(r,t)$ of the c.m. frame self-correlation function $\hat{G}_{\mathrm{mon}}(\mathbf{r},t)$ of the $N = 300$ melt at equilibrium. (b) $\hat{G}^{\mathrm{mon}}_{0,0}(r,t)$ at $\mathrm{Wi_R} = 10$. The solid lines show approximations of the long tails of $\hat{G}^{\mathrm{mon}}_{0,0}(r,t)$ by an exponent function $\exp(-r/\lambda)$. (c) Change of characteristic length λ under steady extensional flow for the $N = 20$ melt. (d) Results for the $N = 300$ melt.

distribution of entanglements along the chain [68]. It follows that λ should increase under flow, as a result of disentanglements, and approach the size of the polymer chain at high strain rates (Fig. 4).

In summary, we propose a framework for the quantitative analysis of polymer self-dynamics under flow, which overcomes the inherent difficulties encountered in the previous attempts [23,25,27,29]. Our method is based on the use of two complementary observation frames and an extension of the spherical harmonic expansion technique to dynamic density correlations. It permits a direct examination of the microscopic dynamics of polymers in steady flow via well-defined space-time correlation functions, without recourse to *ad hoc* algorithms. Application of this approach to NEMD simulations of coarse-grained polymer melts reveals a number of universal features. Lastly, our method is not limited to self-dynamics under uniaxial extension, and should be useful for analysis of shear flows and nonequilibrium single-chain collective dynamics as well.

The research is supported by the U.S. Department of Energy (DOE), Office of Science, Office of Basic Energy Sciences, Early Career Research Program Award No. KC0402010, under Contract No. DE-AC05-00OR22725. The computational work was carried out at Oak Ridge National Laboratory's Center for Nanophase Materials Sciences, which is a DOE Office of Science User Facility. Our investigation used resources of the Oak Ridge Leadership Computing Facility at the Oak Ridge National Laboratory, which is supported by the Office of Science of the U.S. Department of Energy under Contract No. DE-AC05-00OR22725. We thank L. Sanchez-Diaz and W.-R. Chen for their assistance with the simulations.

*wangy@ornl.gov

[1] R. B. Bird and C. F. Curtiss, Fascinating polymeric liquids, Phys. Today **37**, No. 1, 36 (1984).
[2] P.-G. de Gennes, Reptation of a polymer chain in the presence of fixed obstacles, J. Chem. Phys. **55**, 572 (1971).
[3] M. Doi and S. F. Edwards, *The Theory of Polymer Dynamics* (Oxford University Press, Oxford, 1986).
[4] T. McLeish, Tube theory of entangled polymer dynamics, Adv. Phys. **51**, 1379 (2002).
[5] G. Marrucci and B. de Cindio, The stress relaxation of molten PMMA at large deformations and its theoretical interpretation, Rheol. Acta **19**, 68 (1980).
[6] M. Wagner and J. Schaeffer, Nonlinear strain measures for general biaxial extension of polymer melts, J. Rheol. **36**, 1 (1992).
[7] G. Marrucci and G. Iannirubertо, Interchain pressure effect in extensional flows of entangled polymer melts, Macromolecules **37**, 3934 (2004).
[8] R. S. Graham, A. E. Likhtman, T. C. McLeish, and S. T. Milner, Microscopic theory of linear, entangled polymer chains under rapid deformation including chain stretch and convective constraint release, J. Rheol. **47**, 1171 (2003).
[9] J. Qin and S. T. Milner, Tube diameter of oriented and stretched polymer melts, Macromolecules **46**, 1659 (2013).
[10] K. S. Schweizer and D. M. Sussman, A force-level theory of the rheology of entangled rod and chain polymer liquids: I. Tube deformation, microscopic yielding, and the nonlinear elastic limit, J. Chem. Phys. **145**, 214903 (2016).
[11] S.-J. Xie and K. S. Schweizer, Entangled chain polymer liquids under continuous shear deformation: consequences of a microscopically anharmonic confining tube, Soft Matter **14**, 7052 (2018).
[12] R. Yamamoto and A. Onuki, Entanglements in quiescent and sheared polymer melts, Phys. Rev. E **70**, 041801 (2004).
[13] R. Everaers, S. K. Sukumaran, G. S. Grest, C. Svaneborg, A. Sivasubramanian, and K. Kremer, Rheology and microscopic topology of entangled polymeric liquids, Science **303**, 823 (2004).
[14] M. Kröger, Shortest multiple disconnected path for the analysis of entanglements in two-and three-dimensional polymeric systems, Comput. Phys. Commun. **168**, 209 (2005).
[15] C. Tzoumanekas and D. N. Theodorou, Topological analysis of linear polymer melts: A statistical approach, Macromolecules **39**, 4592 (2006).
[16] C. Baig, V. G. Mavrantzas, and M. Kröger, Flow effects on melt structure and entanglement network of linear polymers: Results from a nonequilibrium molecular dynamics simulation study of a polyethylene melt in steady shear, Macromolecules **43**, 6886 (2010).
[17] W. Bisbee, J. Qin, and S. T. Milner, Finding the tube with isoconfigurational averaging, Macromolecules **44**, 8972 (2011).
[18] J. Qin and S. T. Milner, Counting polymer knots to find the entanglement length, Soft Matter **7**, 10676 (2011).

[19] A. E. Likhtman and M. Ponmurugan, Microscopic definition of polymer entanglements, Macromolecules **47**, 1470 (2014).

[20] T. C. O'Connor, N. J. Alvarez, and M. O. Robbins, Relating Chain Conformations to Extensional Stress in Entangled Polymer Melts, Phys. Rev. Lett. **121**, 047801 (2018).

[21] J. P. Boon and S. Yip, *Molecular Hydrodynamics* (Dover Publications, New York, 1991).

[22] T. Van de Ven, Diffusion of Brownian particles in shear flow, J. Colloid Interface Sci. **62**, 352 (1977).

[23] P. Cummings, B. Wang, D. Evans, and K. Fraser, Nonequilibrium molecular dynamics calculation of self-diffusion in a non-Newtonian fluid subject to a Couette strain field, J. Chem. Phys. **94**, 2149 (1991).

[24] R. Yamamoto and A. Onuki, Dynamics of highly supercooled liquids: Heterogeneity, rheology, and diffusion, Phys. Rev. E **58**, 3515 (1998).

[25] J.-P. Ryckaert and C. Pierleoni, Polymer solutions in flow: A non-equilibrium molecular dynamics approach, in *Flexible Polymer Chains in Elongational Flow*, edited by T. Q. Nguyen and H.-H. Kaush (Springer, Berlin, 1999), Chap. 2, pp. 5–40.

[26] L. Berthier and J.-L. Barrat, Shearing a Glassy Material: Numerical Tests of Nonequilibrium Mode-Coupling Approaches and Experimental Proposals, Phys. Rev. Lett. **89**, 095702 (2002).

[27] R. Yamamoto and A. Onuki, Dynamics and rheology of a supercooled polymer melt in shear flow, J. Chem. Phys. **117**, 2359 (2002).

[28] T. A. Hunt and B. Todd, Diffusion of linear polymer melts in shear and extensional flows, J. Chem. Phys. **131**, 054904 (2009).

[29] A. Korolkovas, P. Gutfreund, and M. Wolff, Dynamical structure of entangled polymers simulated under shear flow, J. Chem. Phys. **149**, 074901 (2018).

[30] S. Aime and L. Cipelletti, Probing shear-induced rearrangements in Fourier space: I. Dynamic light scattering, Soft Matter **15**, 200 (2019).

[31] A. Giuntoli, F. Puosi, D. Leporini, F. W. Starr, and J. F. Douglas, Predictive relation for the α-relaxation time of a coarse-grained polymer melt under steady shear, Sci. Adv. **6**, eaaz0777 (2020).

[32] R. P. Pelaez and R. Delgado-Buscalioni, Origin of tank-treading and breathing dynamics of star polymers in shear flow, Macromolecules **53**, 2634 (2020).

[33] D. J. Evans, H. J. Hanley, and S. Hess, Non-Newtonian phenomena in simple fluids, Phys. Today **37**, No. 1, 26 (1984).

[34] Y. Suzuki, J. Haimovich, and T. Egami, Bond-orientational anisotropy in metallic glasses observed by x-ray diffraction, Phys. Rev. B **35**, 2162 (1987).

[35] N. J. Wagner and W. B. Russel, Light scattering measurements of a hard-sphere suspension under shear, Phys. Fluids A **2**, 491 (1990).

[36] Z. Wang, C. N. Lam, W.-R. Chen, W. Wang, J. Liu, Y. Liu, L. Porcar, C. B. Stanley, Z. Zhao, K. Hong, and Y. Wang, Fingerprinting Molecular Relaxation in Deformed Polymers, Phys. Rev. X **7**, 031003 (2017).

[37] C. N. Lam, W.-S. Xu, W.-R. Chen, Z. Wang, C. B. Stanley, Jan-Michael Y. Carrillo, D. Uhrig, W. Wang, K. Hong, Y. Liu, L. Porcar, C. Do, G. S. Smith, B. G. Sumpter, and Y. Wang, Scaling Behavior of Anisotropy Relaxation in Deformed Polymers, Phys. Rev. Lett. **121**, 117801 (2018).

[38] S. Bruzzone and M. Malvaldi, Dynamics of relaxation of entangled polymers in shear flow, J. Chem. Phys. **125**, 064909 (2006).

[39] A. Onuki and K. Kawasaki, Critical phenomena of classical fluids under flow: I. Mean field approximation, Prog. Theor. Phys. **63**, 122 (1980).

[40] Y. Wang, W. Wang, K. Hong, and Y. Liu, Quantification of deformation-induced concentration fluctuations in polymeric liquids by small-angle neutron scattering, Macromolecules **54**, 3531 (2021).

[41] J. Ma, Jan-Michael Y. Carrillo, C. Do, W.-R. Chen, P. Falus, Z. Shen, K. Hong, B. G. Sumpter, and Y. Wang, Spatial correlations of entangled polymer dynamics, Phys. Rev. E **104**, 024503 (2021).

[42] K. Kremer and G. S. Grest, Dynamics of entangled linear polymer melts: A molecular-dynamics simulation, J. Chem. Phys. **92**, 5057 (1990).

[43] H.-P. Hsu and K. Kremer, Static and dynamic properties of large polymer melts in equilibrium, J. Chem. Phys. **144**, 154907 (2016).

[44] D. J. Evans and G. P. Morriss, *Statistical Mechanics of Nonequilibrium Liquids* (Cambridge University Press, Cambridge, England, 2008).

[45] D. A. Nicholson and G. C. Rutledge, Molecular simulation of flow-enhanced nucleation in *n*-eicosane melts under steady shear and uniaxial extension, J. Chem. Phys. **145**, 244903 (2016).

[46] M. Dobson, Periodic boundary conditions for long-time nonequilibrium molecular dynamics simulations of incompressible flows, J. Chem. Phys. **141**, 184103 (2014).

[47] $\tau_0 \approx 2.58$ for current model [48].

[48] T. C. O'Connor, A. Hopkins, and M. O. Robbins, Stress relaxation in highly oriented melts of entangled polymers, Macromolecules **52**, 8540 (2019).

[49] LAMMPS website: http://lammps.sandia.gov.

[50] S. Plimpton, Fast parallel algorithms for short-range molecular dynamics, J. Comput. Phys. **117**, 1 (1995).

[51] W. M. Brown, P. Wang, S. J. Plimpton, and A. N. Tharrington, Implementing molecular dynamics on hybrid high performance computers: Short range forces, Comput. Phys. Commun. **182**, 898 (2011).

[52] See Supplemental Material at http://link.aps.org/supplemental/10.1103/PhysRevLett.129.057801 for details on simulation methods, spherical harmonic expansion analysis, c.m. motions in flow frame, and monomer motions in c.m. frame, which includes Refs. [53–62].

[53] M. Kröger, Efficient hybrid algorithm for the dynamic creation of wormlike chains in solutions, brushes, melts and glasses, Comput. Phys. Commun. **118**, 278 (1999).

[54] S. W. Sides, G. S. Grest, M. J. Stevens, and S. J. Plimpton, Effect of end-tethered polymers on surface adhesion of glassy polymers, J. Polym. Sci. Part B **42**, 199 (2004).

[55] T. A. Hunt, Periodic boundary conditions for the simulation of uniaxial extensional flow of arbitrary duration, Mol. Simul. **42**, 347 (2016).

[56] D. Elrick, Source functions for diffusion in uniform shear flow, Aust. J. Phys. **15**, 283 (1962).

[57] W. Paul, G. D. Smith, D. Y. Yoon, B. Farago, S. Rathgeber, A. Zirkel, L. Willner, and D. Richter, Chain Motion in an Unentangled Polyethylene Melt: A Critical Test of the Rouse Model by Molecular Dynamics Simulations and Neutron Spin Echo Spectroscopy, Phys. Rev. Lett. **80**, 2346 (1998).

[58] G. D. Smith, W. Paul, M. Monkenbusch, and D. Richter, On the non-Gaussianity of chain motion in unentangled polymer melts, J. Chem. Phys. **114**, 4285 (2001).

[59] M.-C. Chang, C.-H. Tung, S.-Y. Chang, J. M. Carrillo, Y. Wang, B. G. Sumpter, G.-R. Huang, C. Do, and W.-R. Chen, A machine learning inversion scheme for determining interaction from scattering, Commun. Phys. **5**, 46 (2022).

[60] S. Hamaguchi, R. T. Farouki, and D. H. E. Dubin, Triple point of Yukawa systems, Phys. Rev. E **56**, 4671 (1997).

[61] M. O. Robbins, K. Kremer, and G. S. Grest, Phase diagram and dynamics of Yukawa systems, J. Chem. Phys. **88**, 3286 (1988).

[62] R. Ullman, Small angle neutron scattering from polymer networks, J. Chem. Phys. **71**, 436 (1979).

[63] S. Hess and J. C. Rainwater, Diffusion in a laminar flow: Shear rate dependence of correlation functions and of effective transport coefficients, J. Chem. Phys. **80**, 1295 (1984).

[64] G. P. Krishnan and D. T. Leighton, Jr., Diffusion from a point source in a time-dependent unbounded extensional flow, Phys. Fluids A **4**, 2327 (1992).

[65] M. Guenza, Cooperative Dynamics in Unentangled Polymer Fluids, Phys. Rev. Lett. **88**, 025901 (2001).

[66] G. Yatsenko, E. J. Sambriski, M. A. Nemirovskaya, and M. Guenza, Analytical Soft-Core Potentials for Macromolecular Fluids and Mixtures, Phys. Rev. Lett. **93**, 257803 (2004).

[67] P. Chaudhuri, L. Berthier, and W. Kob, Universal Nature of Particle Displacements Close to Glass and Jamming Transitions, Phys. Rev. Lett. **99**, 060604 (2007).

[68] B. Wang, J. Guan, S. M. Anthony, S. C. Bae, K. S. Schweizer, and S. Granick, Confining Potential When a Biopolymer Filament Reptates, Phys. Rev. Lett. **104**, 118301 (2010).